Hydrol. Earth Syst. Sci. Discuss., 9, 1–27, 2012
www.hydrol-earth-syst-sci-discuss.net/9/1/2012/
doi:10.5194/hessd-9-1-2012

Hydrology and Earth System Sciences Discussions

Hydrologic and geochemical modeling of a karstic Mediterranean watershed

N. P. Nikolaidis[1], F. Bouraoui[2], and G. Bidoglio[2]

[1]Department of Environmental Engineering, Technical University of Crete, Chania, Greece
[2]Institute for Environment and Sustainability, Joint Research Centre, European Commission, Ispra, Italy

Received: 1 December 2011 – Accepted: 16 December 2011 – Published: 3 January 2012

Correspondence to: N. P. Nikolaidis (nikolaos.nikolaidis@enveng.tuc.gr)

Published by Copernicus Publications on behalf of the European Geosciences Union.

Abstract

The SWAT model was modified to simulate the hydrologic and chemical response of karstic systems and assess the impacts of land use management and climate change of an intensively managed Mediterranean watershed in Crete, Greece. A methodology was developed for the determination of the extended karst area contributing to the spring flow as well as the degree of dilution of nitrates due to permanent karst water volume. The modified SWAT model has been able to capture the temporal variability of both karst flow and surface runoff using high frequency monitoring data collected since 2004 in addition to long term flow time series collected since 1973. The overall hydrologic budget of the karst was estimated and its evaporative losses were calculated to be 28 % suggesting a very high rate of karst infiltration. Nitrate chemistry of the karst was simulated by calibrating a dilution factor allowing for the estimation of the total karstic groundwater volume to approximately 500 million m^3 of reserve water. The nitrate simulation results suggested a significant impact of livestock grazing on the karstic groundwater and on surface water quality. Finally, simulation results for a set of climate change scenarios suggested a 17 % decrease in precipitation, 8 % decrease in ET and 22 % decrease in flow in 2030–2050 compared to 2010–2020. A validated tool for integrated water management of karst areas has been developed, providing policy makers an instrument for water management that could tackle the increasing water scarcity in the island.

1 Introduction

Continuous habitation in the past 12 000 yr of areas prone to water scarcity such as the Mediterranean region has been primarily due to existence of reliable spring water supply derived mostly from karstic formation natural reservoirs as well as the ability of land to regenerate itself (Nikolaidis, 2011; Stamati et al., 2011). Karsts are derived from the dissolution of limestone and dolomite formations and are comprised of

HESSD
9, 1–27, 2012

a high transmissivity fractured system of sinkholes, caves and springs. Such large, below-ground natural reservoirs are very important in water resources management of the Mediterranean region because they regulate water discharge of the karstic springs throughout the year (Moraetis et al., 2010; Kourgialas et al., 2010). These water bodies will play a significant role in the overall rational management of water resources of climate change impacted transitional areas such as the Mediterranean where the precipitation is expected to decrease by at least 25 % with increases in the frequency of extreme events and the average annual temperature to increase from 2–4 °C according to the IPPC (2007) scenarios. Warmer and drier conditions are expected to intensify water shortages and cause loss in biodiversity and ecosystem services (Nikolaidis, 2011).

The importance of karstic aquifers in regional water management has been recognized by the European Union (which prompted the creation of COST Action 620 to develop a comprehensive risk based methodology for the sustainable management of karstic systems) and the US EPA (which recognized the contribution of karst areas on the hydrology of ephemeral and intermittent streams) and prompted the development of tools for sustainable management (EC, 2003; Levick et al., 2008). These water bodies will play a major role in water management as they relate to water availability for potable water and agriculture (ie. food security issues). Agriculture is a major driver in the management of water especially in Mediterranean (Albiac et al., 2006; Wriedt et al., 2009) where 75 % of the total area is irrigated and it accounts for more than 60 % of the total water abstractions (e.g. Spain 64 %, Greece 88 %, Portugal 80 %).

During the past five years, a variety of karst models have been developed and applied to karst formation discharge in Europe, North America and Asia. Rozos and Koutsoyiannis (2006) conceptualized conduit flow using Manning's equation and developed a multi-cell model consisting of reservoirs and conduits in 3-D. The model was applied to Almyros spring data (Eastern Crete, Greece) and the simulation results were compared with simulations of MODFLOW. Similar comparison of a lumped karst model with Visual MODFLOW was also conducted by Martinez-Santos and Andreu (2010).

HESSD
9, 1–27, 2012

Fleury et al. (2007) used a three reservoir model to simulate successfully soil, slow discharge and rapid discharge of Fontaine de Vaucluse karstic aquifer in Southern France. A modified version of this model was used to simulate Lez spring by incorporating active groundwater management (Fleury et al., 2009). A further improvement of such model was the incorporation of non-linear hysteretic discharge functions that were applied to Vensim model by Tritz et al. (2011). Zhang et al. (2011) modified a Distributed Hydrologic-Soil-Vegetation Model (DHSVM) to include flow routing in karst conduits and model the hydrologic response of a small karst basin in southwest China. Other distributed approaches to modeling karst hydrology were presented by Smaoui et al. (2011) that used the HySuf-FEM (Hydrodynamic of Subsurface Flow by Finite Element Method) code to model the Berrechid karst aquifer in Morocco as well as Kurtulus and Razack (2010) that used artificial neural network and adaptive neuro-fuzzy interface system to model the daily discharge of the La Rochefoucauld karst aquifer in South-Western France.

Distributed parameter watershed models such as SWAT (Soil and Water Assessment Tool, Arnold et al., 1998) and HSPF (Hydrologic Simulation Program – FORTRAN, Bicknell et al., 2001) have been used in the past to simulate the hydrologic response of karstic formations (Spruill et al., 2000; Refsgaard, 1997). Tzoraki and Nikolaidis (2007) developed a two linear reservoir model to simulate the karst and combined it with HSPF to simulate the hydrology, sediment transport and nutrient loads of Krathis River basin in Northern Peloponnese, Greece. Kourgialas et al. (2010) added a distributed snow model to the karstic two reservoir model and combined it with HSPF in order to simulate the hydrologic response of the Koiliaris River basin in Crete, Greece. Afinowicz et al. (2005) modified the aquifer discharge parameterization of the SWAT model in order to better simulate the quick flow response of the karst in Texas and Baffaut and Benson (2009) extended this parameterization by including sinkholes, losing streams and return flow to model flow, fecal coliforms and phosphorus in a Missouri karstic watershed.

HESSD
9, 1–27, 2012

The peculiarity of Mediterranean karst systems relies on the fact that a spring could receive contributions from the karst that it is extended outside the watershed boundaries to which the spring belongs to as well as karsts situated one on top of the other with different hydraulic characteristics and thus different transmissivities (EC 2004). Identification of the extended karst area that contributes to the flow of the spring is extremely important in order to obtain accurate hydrologic and geochemical balances of the system (Tzoraki and Nikolaidis, 2007; Moraetis et al., 2010; Kourgialas et al., 2010). A second peculiarity in the behavior of karstic system under pressure has been discussed in detailed by Moraeitis et al. (2010) and deals with the diurnal variation of karst level. Barometric and temperature changes at the entrance of the sinkhole create changes to the barometric pressure above the water table of the karst, making it to operate as a bladder pump and introducing energy into the system which is transformed into a highly dispersive system causing mixing and dilution of the pollutants. Modeling of the geochemistry of the karst requires the determination of the degree of dilution i.e. volume of water within the karst below the level of spring discharge.

The objective of this research was to study the hydrologic and chemical response of a karst system in an intensively managed Mediterranean watershed in Crete, Greece and then assess the impacts of land use management and climate change on the hydrologic and chemical regime of the watershed. The SWAT model was modified to model the hydrologic and chemical response of karst providing in this way policy makers a validated tool for integrated water management that would tackle the increasing water scarcity in the island. We have selected to model the nitrogen cycle as an indicator of both livestock and cultivation impacts on surface and groundwater quality (Glibert et al., 2006). Proper management of the nitrogen cycle in intensively managed areas has become an urgent priority since it appears that nitrogen is one of the planetary boundaries for safe operating space for humanity that has been exceeded (Rockstrom et al., 2009).

HESSD
9, 1–27, 2012

2 Watershed description and available data

Koiliaris River watershed is located in the north-western part of Crete near Chania, Greece and has a watershed area of 130 km^2 (Fig. 1). Based on the geomorphologic characteristics of the basin, hydrologic modeling and the orientation of the fault system, the extended karst area that contributes to the spring flow in the watershed was located south east of the area and was estimated to include at least 50 km^2 (Moraetis et al., 2010). The watershed has an intense geomorphology with elevations ranging from 0 to 2120 m a.s.l. and slopes ranging from 43 % (at high elevations) to 1–2 % (valley). The predominant geologic formations are: limestones, dolomites, marbles, and re-crystallized limestones with cherts of the Plattenkalk, Tripolis, and Trypali series (71.8 %), calcaric marls and marls – Neogene deposits (15.6 %), schists (6.1 %) and quaternary alluvial deposits (6.4 %). There are two episodic and one temporary tributaries in the basin and they are joined by Stylos spring discharge to make the permanent reach of Koiliaris River. The two episodic tributaries drain the karst area (north-east part of the watershed), while the episodic tributary flows initially over schist formations before it enters a karstic gorge situated along a fault (Diktamos Gorge). The confluence of the three tributaries is located in the alluvial deposits of the valley. The karstic system of the basin is comprised of two geologic formations: the Limestones of Trypalis zone (Triassic to Cretaceous period) and the autochthonous Metamorphic Crystalline Limestones (Plattenkalk–Mesozoic period) with different hydraulic characteristics (faster and slower response, respectively).

The agricultural land consists of olive groves, citrus groves, vines and vegetables (32.1 %) grown with conventional practices such as tilling, irrigation and use of fertilizers. Intensively grazed scrubland/pasture by livestock covers large areas (67.3 %) of the watershed at high altitudes and forest (0.6 %). The composition of land use has not changed in the past 50 yr, however, the intensity of use has changed significantly. For instance, the number of animals grazing in the watershed and its extended karst increased from about 23 393 sheeps and goats in 1961 to 123 987 in 2001. Since the grazing area remained relatively constant (16 875 ha), the grazing intensity changed from a level of 1.4–6.8 animals ha^{-1}. Similarly, the cultivation of agricultural land has been intensified with increasing fertilizer application. Using country statistics, fertilizer consumption rose steadily from 159 000 $t\,yr^{-1}$ in 1960 to 710 000 $t\,yr^{-1}$ in 1990 and then it has been dropping to 405 000 $t\,yr^{-1}$ in 2002. Intensive cultivation and livestock grazing have deteriorated significantly soil quality and land fertility. Soils are thin, poorly developed, following the lithology of the area. There are three main types of soils: in high altitude, there are calcaric Lithosols (FAO) obtained from the weathering of limestones, the calcaric regosols developed in low altitudes in Neocene and Alluvial formations and the eutric lithosols developed in schists with mainly coarse texture.

The Region of Crete in collaboration with the Prefecture of Chania have been conducting meteorological and hydrologic monitoring of precipitation (daily), air temperature (daily), spring flow (on a monthly basis) since 1973. The Technical University of Crete augmented this network and in 2004 initiated hydrologic and geochemical monitoring of the Basin consisting of a continuous telemetric monitoring gauging station (5 min to 1 h interval) in Koiliaris river (R1), level loggers at the entrance and exit of the gorge (R2 and R3), water level and temperature logger at the Macheri well (G1) and two meteorological stations (M1 and M2) at elevations of 950 and 300 m a.s.l. (Fig. 1). The sensors included in the telemetric gauging station (R1) include pH, nitrate (NO_3^--N), water temperature (°C), dissolved oxygen ($mg\,l^{-1}$) and river stage (m) (multi-parameter Troll9500 by In Situ Inc.). In addition to the telemetric data, monthly field campaigns are conducted for both surface and groundwater quality measurements. Further details on the monitoring network and data analysis can be found in Moraetis et al. (2010).

3 SWAT model description and modifications

SWAT is a deterministic, continuous time (daily time step) basin scale model that was designed to simulate the hydrology, sediment yield and water quality (nutrient and pesticides) of ungauged watersheds (Arnold et al., 1998) and evaluate the impact of

HESSD
9, 1–27, 2012

agricultural management practices on water quality and agricultural yields. The watershed is first subdivided into subcatchments and each subcatchment into hydrologic response units (HRU) that are a function of soil type, land use and land slope. The model has incorporated the following components: weather generator routine, hydrologic mass balance, soil temperature and soil properties, plant growth, nutrients, pesticides, bacteria and pathogen mass balances, and land management practices. The hydrologic component of each HRU includes the following processes: evapotranspiration, plant uptake, surface runoff and infiltration (using the modified Curve Number or the Green-Ampt method), percolation, lateral subsurface flow, groundwater return flow from the shallow aquifer, deep aquifer losses and channel transmission loss subroutines. Water balance is conducted for the snow compartment, soil, shallow aquifer and deep aquifer. Plant growth is based on the EPIC crop model and uses the "heat units" concept which relates crop growth to the excess of daily temperature above a base temperature. Potential evapotranspiration, leaf area index, rooting depth and soil water content determine the water uptake of plants.

In order to be able to simulate the contribution of the extended karst to the discharge of a spring as well as account for the variability of the recession of the discharge due to two karst formations, we augmented SWAT by using (in series) a modified version of the karst flow model described by Tzoraki and Nikolaidis (2007) and Kourgialas et al. (2010). A brief description of the modified karst model follows. The major modifications from the previous versions are: (a) the input flow is the deep groundwater flow from SWAT and (b) a nitrate-N mass balance was included assuming that nitrate is conservative in the karst. The hydrologic mass balances of the karst model are:

Upper reservoir mass balance

$$\frac{dV_1}{dt} = Q_{\text{in},1} - Q_1 \quad (1)$$

Lower reservoir mass balance

$$\frac{dV_2}{dt} = Q_{\text{in},2} - Q_2 \quad (2)$$

HESSD
9, 1–27, 2012

where $Q_{in,1} = a_1 \cdot Q_{in,deepGW}$, $Q_{in,2} = (1-a_1)\cdot Q_{in,deepGW} + a_2 \cdot Q_1$, $Q_1 = K_u \cdot V_1$, $Q_2 = K_l \cdot V_2$, and $Q_{in,deepGW}$ is the deep groundwater flow from SWAT, a_1 is the fraction of karst with the upper reservoir, a_2 is the fraction of flow from the upper reservoir discharge entering the lower reservoir and K_u and K_l are recession constants ($1/d$) for the upper and lower reservoir. For constant $Q_{in,1}$ and $Q_{in,2}$ (daily time step) the analytical solutions of 1 and 2 follow:

$$Q_1 = Q_{1,0}e^{-k_u t} + Q_{in,1}(1-e^{-k_u t}) \tag{3}$$

$$Q_2 = Q_{2,0}e^{-k_l(1-a_2)t} + (1-a_1)Q_{in,2}(1-e^{-k_l(1-a_2)t}) \tag{4}$$

The total karstic flow is calculated as:

$$Q_{karstic} = (1-a_2)Q_1 + Q_2 \tag{5}$$

In a similar fashion, the nitrate-N mass balances are:
Upper reservoir mass balance

$$\frac{d(V_1 \cdot C_1)}{dt} = a_1 \cdot Q_{in,1} \cdot C_{in,1} - Q_1 \cdot C_1 \tag{6}$$

Lower reservoir mass balance

$$\frac{d(V_2 \cdot C_2)}{dt} = (1-a_1)\cdot Q_{in} \cdot C_{in,} + a_2 \cdot Q_1 \cdot C_1 - Q_2 \cdot C_2 \tag{7}$$

The mass balance equations were solved analytically for a daily input time step. Given that the volume of the two reservoirs reflect the daily volume corresponding to the discharging water from the spring and does not account for the permanent volume of the karst below the spring level, a deep karst factor was introduced in the model to account for the extra dilution of the incoming chemical loads and in this way provide an estimate of the total volume of the karst. Moraetis et al. (2010) discussed in detail the fluctuation of the karst water level which introduces significant dispersion in the system and thus mixing of the incoming loads.

HESSD
9, 1–27, 2012

An excel version of the karstic model was used for this study in order to facilitate model calibration as well as sensitivity and uncertainty analysis. The precipitation in the karst region of the watershed was directed to deep groundwater after allowing SWAT to simulate surface hydrologic processes such as snow accumulation and melt, surface runoff, infiltration to shallow groundwater and evapotranspiration. The deep groundwater flow of the karstic region that could be attributed to a specific spring (based on fault analysis and other available data and observations) was aggregated on a daily basis and was input to the two-part reservoir karst model. The karst model parameters were calibrated and the resulting time series were used as point source input at the spring. The extended karst contributing area was determined by trial and error, i.e. including or excluding different HRUs deep groundwater flows. Once the karst model parameters were calibrated, the excel could be connected to a risk analysis software (@RISK by PALISADE) to conduct easily sensitivity and uncertainty analysis due to model parameters.

Three years of hydrologic and water quality data from 2007 until 2010 were used in order to calibrate the model. The data included a complete data set of flow measurements at the watershed outlet, flow data of Keramianos tributary at the gorge entrance and exit for 2007–2008, grab sample data for nitrates at Keramianos tributary, the watershed outlet and groundwater wells and continuous high frequency nitrate data (converted to flow weighted daily average values) at the watershed outlet. The verification of the hydrologic calibration was obtained using watershed data from 2004 to 2007 as well as spring flow monthly measurements from 1973 to 2004 for two out of the three springs of the watershed. The two springs measured are located at the community of Stylos and the third spring (Anavreti) at the community of Nio Chorio. Anavreti is an intermittent spring that runs for a few months between December and March. Existing nitrate grab sample measurements between 2004 and 2007 were used for the verification of the nitrate simulation.

The methodology used for model calibration followed a three step approach. First the hydrologic parameters of the subbasins contributing to Keramianos tributary surface

HESSD
9, 1–27, 2012

runoff were calibrated. Then the transmission losses through the gorge were adjusted and finally, the Stylos spring flow was calibrated using the methodology outlined earlier for the determination of the extended karst.

4 Results and discussion

The region was delineated into 41 subbasins using as criterion the elemental catchment of 500 ha and 160 hydrologic response units (HRUs). The immediate Koiliaris catchment had a surface area of 132 km^2 and it was divided into 8 subbasins and 27 HRUs while the contributing extended karst had a surface area of 79 km^2 (11 subbasins and 28 HRUs). Time series from 6 precipitation stations were used to synthesize 37 yr of precipitation record (1973–2010) by filling missing data using cross station regressions. The density of the precipitation network and the location of the stations (3 within the watershed at 3 different elevations and 3 stations outside the watershed) were able to account for the orographic variability of rainfall. On the other hand, a 37 yr long record was synthesized for two temperature stations and a temperature gradient of $-5.6\,^{\circ}$C/1000 m elevation was used to adjust the daily temperature record in every subbasin and account for the orographic effect. The elevation band feature of the SWAT model was activated in order to better capture the snow/rain distribution in the basin.

4.1 Hydrologic simulation

The annual areal weighted precipitation for the calibration period over the watershed and the extended contributing karst was 1363 mm yr^{-1} while the actual evapotraspiration was estimated to be 455 mm yr^{-1}. Snow covered an area of 82 km^2 and melted within a few days at low elevations and 100–140 days at high elevations, respectively. Snow cover typically started in early December and lasted until early May. The annual average outflow of Koiliaris River Basin was estimated to be 621 mm yr^{-1}

($131\,\mathrm{Mm^3\,yr^{-1}}$). A comparison between simulated flows and observed flows at three stations in the watershed is presented in Fig. 2. The annual average flow at the gorge entrance was estimated to be $12.5\,\mathrm{Mm^3\,yr^{-1}}$. Using 240 days daily flow data, the root mean squared error (RMSE) was estimated to be $0.087\,\mathrm{m^3\,s^{-1}}$ and the closure of the cumulative simulated flow and observed flow was 15 %. The annual average flow at the gorge exit was estimated to be $2.2\,\mathrm{Mm^3\,yr^{-1}}$ due to transmission losses. The RMSE was estimated to be $0.048\,\mathrm{m^3\,s^{-1}}$. Finally, the annual average flow at the basin's outlet (Koiliaris gauging station) was estimated to be $131\,\mathrm{Mm^3\,yr^{-1}}$, $118\,\mathrm{Mm^3\,yr^{-1}}$ from Karst and $13\,\mathrm{Mm^3\,yr^{-1}}$ from surface runoff. The RMSE was estimated to be $2.9\,\mathrm{m^3\,s^{-1}}$ and the closure of the cumulative simulated flow and observed flow was 2.6 %. The mean daily observed flow was $4.25\,\mathrm{m^3\,s^{-1}}$ ($5.32\,\mathrm{m^3\,s^{-1}}$ standard deviation) while the mean daily simulated flow was $4.14\,\mathrm{m^3\,s^{-1}}$ ($5.24\,\mathrm{m^3\,s^{-1}}$ standard deviation). The coefficient of determination between observed and simulated flows was 0.72 and the slope 0.89. The goodness of fit of the calibration period was examined using the statistics suggested by Moriasi et al. (2007), namely the Nash-Sutcliffe Efficiency (NSE), Percent Bias (PBias), and RMSE Standard Deviation Error (RSR). A simulation is considered adequate if $\mathrm{NSE} > 0.5$, $\mathrm{PBias} < \pm 25\,\%$ and $\mathrm{RSR} < 0.7$. These statistics were calculated using the daily record and the monthly average record. The NSE was 0.62, PBias −22.3 and RSR 0.62 for the daily record and 0.77, −22.1 and 0.48 for the monthly record. The goodness of fit of the calibration was considered adequate since all three statistics were passed for both daily and monthly record.

The overall hydrologic budget of Keramianos sub-basin that is characteristic mostly of a schist geologic bedrock was the following. The annual average precipitation and snow melt was $1209\,\mathrm{mm\,yr^{-1}}$, ET was $567\,\mathrm{mm\,yr^{-1}}$ and the runoff was $547\,\mathrm{mm\,yr^{-1}}$. The runoff coefficient of the basin was 45 %. The overall hydrologic budget of the karst was the following. The annual average precipitation and snow melt was $1494\,\mathrm{mm\,yr^{-1}}$, ET was $418\,\mathrm{mm\,yr^{-1}}$ and the spring runoff was $803\,\mathrm{mm\,yr^{-1}}$. The runoff coefficient of the karst was estimated to be 54 %. The evaporative losses of the karst were estimated to be 28 % suggesting a very high rate of karst infiltration which could be justified by

HESSD
9, 1–27, 2012

the very thin soils, sparse vegetation at high elevation and intense karstification of the Tripali zone.

Model verification was achieved using an independent record of flows (2004–2007) and simulating the whole basin. A comparison between simulated flows and observed flows at the Koiliaris gaging station is presented in Fig. 3. The goodness of fit statistics of the verification period were the following. The NSE was 0.43, PBias – 11.6 and RSR 0.75 for the daily record and 0.61, −11.8 and 0.63 for the monthly record. The goodness of fit of the verification simulation was considered adequate for the monthly record since all three statistics were passed, but not for the daily record. In addition, a qualitative verification of the hydrologic simulation was conducted using monthly flow measurements since 1973 of two of the three outlet points of the Stylos spring. The simulated flows compare very well with the observed data for 8–9 out of the 12 months confirming the goodness of fit of the hydrologic simulation using this long term record.

A sensitivity and uncertainty analysis was conducted by combining the karstic model with @RISK, a risk analysis software in order to determine the uncertainty of the four model parameters controlling discharge. We assumed that the parameter had a uniform distribution ±50 % of their respective calibrated value. We run 1000 Monte Carlo simulations and calculated the distributions on the monthly average discharge for 2008–2009 hydrologic year. The most sensitive parameters in ranking order were: K_l, the recession constants for the lower reservoir, a_2, the fraction of flow from the upper reservoir discharge entering the lower reservoir, a_1, the fraction of karst with the upper reservoir, and K_u, the recession constants for the upper reservoir. The uncertainty (95 % confidence level) of the simulation results due to model parameters ranged from 0.2–5.8 % of the monthly average discharge.

4.2 Nitrate simulation

Nitrogen inputs in the watershed and its extended karst were calculated as follows. Nitrate-N atmospheric deposition was estimated to 11.5 kg ha^{-1} yr^{-1} using a measured average rainfall concentration for nitrate-N of 0.91 mg l^{-1} and a dry

HESSD
9, 1–27, 2012

deposition of inorganic nitrogen of 6 kg ha^{-1} yr^{-1}. Inorganic fertilization and livestock manure contributed 18.3, 10.1 and 17.4 kg ha^{-1} yr^{-1} of nitrate-N, ammonia-N and organic-N, respectively. Inorganic fertilization was applied (using a 30–15-0 fertilizer) at a rate of 80 kg ha^{-1} for olive groves, 70 kg ha^{-1} for citrus and vines and 220 kg ha^{-1} for other crops. Manure was applied to pasture and forested areas depending on the livestock density using OECD excretion rates of 10 kg-N head^{-1} yr^{-1} and 260 kg manure head^{-1} yr^{-1} for sheeps and goats. The application rates were estimated then to be 110 kg ha^{-1} mo^{-1} in the municipality of Armenoi, 150 kg ha^{-1} mo^{-1} in the municipalities of Fre and Krionerida and 200 kg ha^{-1} mo^{-1} in the municipality of Kearmia. Nitrate uptake was estimated to be 41.94 kg ha^{-1} from the simulation. Nitrate-N export to the sea was estimated to be 284 t yr^{-1} or 13.5 kg ha^{-1} yr^{-1}. A comparison of the simulated nitrate concentration at the gorge entrance and at the basin's outlet (Koiliaris gaging station) is presented in Fig. 4. In order to simulate the chemistry of the karst, for the reasons explained earlier in the model development, a dilution factor was assumed of 4.5. This means that the total volume of the karstic reservoir is 4.5 times the annual flow of the springs. This brings the estimate of the total groundwater volume within the watershed and the extended karst contributing to the spring to approximately 500 million m^3 of reserve water. There are very few grab sample data to compare with the simulation results at the entrance of the gorge, however, the simulation has captured the variability of the data. A better statistical analysis of the results was conducted at the main gaging station. The mean daily observed nitrate concentration was 1.2 mg l^{-1} (0.56 mg l^{-1} standard deviation) while the mean daily simulated nitrate concentration was 1.11 mg l^{-1} (0.41 mg l^{-1} standard deviation). The RMSE of the simulation was 0.57 mg l^{-1}. The nitrate simulation passed through ± one standard deviation of the observed data 80 % of the time on a monthly basis. The results suggest a significant impact of livestock grazing on the karstic groundwater and on surface water quality. Livestock manure accumulates on the soil/karst surface during the dry period and it is flushed out during the first rainfall events in the fall, raising the nitrate-N concentrations in groundwater to 8 mg l^{-1}.

HESSD
9, 1–27, 2012

The uncertainty (95 % confidence level) of the simulation results of nitrate concentrations due to model the four hydrologic parameters and one chemical parameter (deep karst factor) was very low and on average 0.12 % of the monthly average nitrate concentration.

4.3 Hydrologic hindcasting simulations

A trend analysis of precipitation, temperature and flow for the existing 37 yr record showed the following. There has been a decreasing trend in precipitation on an annual basis as well as three out of the six wet months (October, January and March). The maximum temperature has no trend on an annual basis and increasing trend for the months of August through October and decreasing for January and February. The minimum temperature has an increasing trend on an annual basis as well as for all the months of the year.

The SWAT model has simulated 74 flood events at the gorge exit. Figure 5a presents the daily simulated hydrograph at that location. The frequency distribution of flood events has not changed with time however, the intensity of the flood has changed significantly through the years. Prior to the drought years of 1988 and 1991 (1973–1992), there were 37 flood events with average maximum flood flow at the exit of the gorge of 1.7 $m^3 s^{-1}$, while from 1993–2010, there were 38 flood events with average maximum flood flow of 4.3 $m^3 s^{-1}$ (2.5 times higher). Figure 5b presents the frequency distribution of maximum flood flows at the same location using all flood events and Fig. 5c presents the distributions for two distinct periods, 1973–1996 and 1997–2010. There has been a significant shift in the frequency of the maximum floods towards higher intensity, which is in agreement with the trend analysis of precipitation and temperature.

4.4 Future scenarios

Figure 6 presents the predictions of annual precipitation, actual ET and runoff for Koiliaris River Basin under the (a) BCM_RCA, (b) ECHAM_RACMO, and

HESSD
9, 1–27, 2012

(c) ECHAM_REMO climate change scenarios for the 1990–2050. All three scenarios give consistent results, predicting significant decreases in annual precipitation, actual ET and runoff after 2030. In order to quantify the changes due to climate, given the local decadal climatic variability, we calculated 20-yr average (and standard deviation) from the three climate change scenarios for precipitation, actual ET and flow for Koiliaris River Basin (based on model simulations, see Fig. 7). The results suggest a 17 % decrease in precipitation, 8 % decrease in ET and 22 % decrease in flow in 2030–2050 compared to 2010–2020. Climate change will exacerbate the problem of water scarcity in the region that will be pronounced in the summer months.

5 Conclusions

The modified SWAT model has been able to capture the temporal variability of both karstic flow and surface runoff using high frequency monitoring data collected since 2004, the long term flow time series collected since 1973 as well as the variability of nitrate concentrations as a proxy to land use impacts. The results of this study can be summarized as follows:

- The overall hydrologic budget of the karst was estimated and its evaporative losses were 28 % suggesting a very high rate of karst infiltration.
- Nitrate chemistry of the karst was simulated by calibrating a dilution factor (4.5) which allowed for the estimation of the total karstic groundwater volume to approximately 500 million m^3 of reserve water. The nitrate simulation results suggested a significant impact of livestock grazing on the karstic groundwater and on surface water quality. Livestock manure accumulated on the soil/karst surface during the dry period and it is flushed out during the first rainfall events in the fall, raising the nitrate-N concentrations in groundwater to 8 mg l^{-1}. In addition, nitrate-N export to the sea was estimated to be 284 t yr^{-1} or 13.5 kg ha^{-1} yr^{-1} impacting the coastal zone.

HESSD
9, 1–27, 2012

- The SWAT model simulated successfully 74 flush flood events that occurred in 37 yr. There has been a significant shift in the frequency of the maximum floods towards higher intensity (1973–1996 vs. 1997–2010), which is in agreement with the trend analysis of precipitation and temperature.
- Finally, climate change simulation results suggested a 17 % decrease in precipitation, 8 % decrease in ET and 22 % decrease in flow in 2030–2050 compared to 2010–2020. Climate change will exacerbate the problem of water scarcity in the region that will be pronounced in the summer months.

This study has shown that Koiliaris River Basin is already experiencing the impacts of climate change in the past 50 yr while land use practices (especially of livestock grazing) have impacted adversely surface and groundwater quality. A validated tool for integrated water management has been developed, providing policy makers with an instrument for water management that could tackle the expected decrease of water availability in the Koiliaris River basin and the increasing water scarcity in the island.

Acknowledgements. Funding for this work was provided by the EU FP7-ENV-2009 Project Soil-TrEC "Soil Transformations in European Catchments" (Grant #244118). This work was conducted at the Institute for Environment and Sustainability of the Joint Research Centre (JRC) of the European Commission. N. P. Nikolaidis is grateful for the Technical University of Crete financial support of his sabbatical leave at the JRC.

References

Afinowicz, J. D., Munster, C. L., and Wilcox, B. P.: Modeling effects of brush management on the rangeland water budget: Edwards Plateau, Texas, JAWRA, 41, 181–193, 2005.

Albiac, J., Martinez, Y., and Tapia, J.: Water quantity and quality issues in the Mediterranean agriculture, in: OECD Workshop on Agriculture and Water Sustainability, Markets and Policies, Session 2, 2006.

Arnold, J. G., Srinivasan, R., Muttiah, R. S., and Williams, J. R.: Large-area hydrologic modeling and assessment: Part I. Model development, J. Am. Water Res. Assoc., 34, 73–89, 1998.
Baffaut, C. and Benson, V. W.: Modeling flow and pollutant transport in a karst watershed with SWAT, T. ASABE, 52, 469–479, 2009.
Bicknell, B. R., Imhoff, J. S., Kittle, J. L., Jobes, T. H., and Donigian, A. S.: Hydrological Simulation Program – FORTRAN (HSPF): User's Manual – Version 12, National Exposure Research Laboratory, Office of Research and Development, US Environmental Protection Agency, Athens, Georgia, USA, 2001.
Debele, B., Srinivasan, R., and Parlange, J.-Y.: Hourly Analyses of hydrological and water quality simulations using the ESWAT Model, Water Res. Manage., 23, 303–324, 2008.
Déqué, M., Dreveton, C., Braun, A., and Cariolle, D.: The ARPEGE/IFS atmosphere model: a contribution to the French community climate modeling, Clim. Dynam., 10, 249–266, 1994.
EC: Vulnerability and risk mapping for the protection of carbonate (Karst) aquifers, edited by: Zwahlen, F., COST-620 Action Final Report, European Commission, DG-Research, 320 pp., 2003.
EC: The main coastal karstic aquifers of Southern Europe, edited by: Calaforra, J. M., COST-621 Action "Groundwater management of coastal karstic aquifers", European Commission, DG-Research, 126 pp., 2004.
Fleury, P., Plagnes, V., and Bakalowicz, M.: Modelling the functioning of karst aquifers with a reservoir model: application to Fontaine de Vaucluse (South of France), J. Hydrol., 345, 38–49, 2007.
Fleury, P., Ladouche, B., Conroux, Y., Jourde, H., and Dorfliger, N.: Modelling the hydrologic functions of a karst aquifer under active water management – the Lez spring, J. Hydrol., 365, 235–243, 2009.
Glibert, P. M., Harrison, J., Heil, C., and Seitzinger, S.: Escalating worldwide use of urea – a global change contributing to coastal eutrophication, Biogeochemistry, 77, 441–463, 2006.
IPCC: Emissions scenarios, A special report of Working Group III of the International Pannel on Climate Change, edited by: Nakicenovic, N. and Swart, R., Cambridge University Press, 2000.
Jacob, D.: The role of water vapor in the atmosphere, A short overview from a climate modeller's point of view, Phys. Chem. Earth A, 26, 523–527, 2001.
Kjellström, E., Bärring, L., Gollvik, S., and Hansson, U.: A 140-year simulation of European climate with the new version of the Rossby Centre regional atmospheric climate model (RCA3),

HESSD
9, 1–27, 2012

Rep. Meteorol. Climatol., 108, SMHI, Norrköping, Sweden, 2005.
Kourgialas, N. N., Karatzas, G. P., and Nikolaidis, N. P.: An integrated framework for the hydrologic simulation of a complex geomorphological river basin, J. Hydrol., 381, 308–321, 2010.
Kourtulus, B. and Razack, M.: Modeling daily discharge responses of a large karstic aquifer using soft computing methods: Artificial neural network and neuro-fuzzy, J. Hydrol., 381, 101–111, 2010.
Levick, L., Fonseca, J., Goodrich, D., Hernandez, M., Semmens, S., Stromberg, J., Leidy, R., Scianni, M., Guertin, D. P., Tluczek, M., and Kepner, W.: The ecological and hydrological significance of ephemeral and intermittent streams in the arid and semi-arid American Southwest, US Environmental Protection Agency and USDA/ARS Southwest Watershed Research Center, EPA/600/R-08/134, ARS/233046, 116 pp., 2008.
Martinez-Santos, P. and Andreu, J. M.: Lumped and distributed approaches to model natural recharge in semiarid karst aquifers, J. Hydrol., 388, 389–398, 2010.
Moraetis, D., Efstathiou, D., Stamati, F., Tzoraki, O., Nikolaidis, N. P., Schnoor, J. L., and Vozinakis, K.: High frequency monitoring for the identification of hydrological and biochemical processes in a Mediterranean river basin, J. Hydrol., 389, 127–136, 2010.
Moraetis, D., Stamati, F., Kotronakis, E., Fragia, T., Paranychnianakis, N., and Nikolaidis, N. P.: Identification of hydrologic and geochemical pathways using high frequency sampling, REE aqueous sampling and soil characterization at Koiliaris critical zone observatory, Appl. Geochem., 26, S101–S104, 2011.
Nikolaidis, N. P.: Human impacts on soil: Tipping points and knowledge gaps, Appl. Geochem., 26, S230–S233, 2011.
Nikolaidis, N. P., Karageorgis, A., Kapimalis, V., Drakopoulou, P., Skoulikidis, N., Behrendt, H., and Levkov, Z.: Management of nutrient emissions of Axios river catchment: their effect in the coastal zone of Thermaikos gulf-Greece, Ecol. Model., 220, 383–396, 2009.
Refsgaard, J. C.: Parameterisation, calibration and validation of distributed hydrological models, J. Hydrol., 198, 69–97, 1997.
Rockstrom, J., Steffen, W., Noone, K., Persson, E., Chapin, F. S., Lambin, E. F., Lenton, T. M., Scheffer, M., Folke, C., Schellnhuber, H. J., Nykvist, B., de Wit, C. A., Hughes, T., van der Leeuw, S., Rodhe, H., Sorlin, S., Snyder, P. K., Costanza, R., Svedin, U., Falkenmark, M., Karlberg, L., Corell, R. W., Fabry, V. J., Hansen, J., Walker, B., Liverman, D., Richardson, K., Crutzen, P., and Foley, J. A.: A safe operating space for humanity, Nature, 461, 472–475,

2009.
Roeckner, E.: The atmospheric general circulation model ECHAM5. Part 1: Model description, Max Planck Institute for Meteorology Rep. 349, Hamburg, Germany, 127 pp., 2003.
Rojas, R., Feyen, L., Dosio, A., and Bavera, D.: Improving pan-European hydrological simulation of extreme events through statistical bias correction of RCM-driven climate simulations, Hydrol. Earth Syst. Sci., 15, 2599–2620, doi:10.5194/hess-15-2599-2011, 2011.
Rozos, E. and Koutsoyiannis, D.: A multicell karstic aquifer model with alternative flow equations, J. Hydrol., 325, 340–355, 2006.
Smaoui, H., Zouhri, L., Ouahsine, A., and Carlier, E.: Modelling of groundwater flow in heterogeneous porous media by finite element method, Hydrol. Process., doi:10.1002/hyp.8156, in press, 2011.
Spruill, C. A., Workman, S. R., and Taraba J. L.: Simulation of daily and monthly stream discharge from small watersheds using the SWAT model, T. ASAE, 43, 1431–1439, 2000.
Stamati, F., Nikolaidis, N. P., Venieri, D., Psillakis, E., and Kalogerakis, N.: Dissolved organic nitrogen as an indicator of livestock impacts on soil biochemical quality, Appl. Geochem., 26, S340–S343, 2011.
Stamati, F. E., Nikolaidis, N. P., and Schnoor, J. P.: Modeling topsoil carbon sequestration in two contrasting agricultural soils – calibration issues and uncertainty analysis, AGEE, in review, 2011.
Tritz, S., Guinot, V., and Jourde, H.: Modelling the behavious of a karst system catchment using non-linear hysteretic conceptual model, J. Hydrol., 397, 250–262, 2011.
Tzoraki, O. and Nikolaidis, N. P.: A generalized framework for modeling the hydrologic and biogeochemical response of a Mediterranean temporary river basin, J. Hydrol., 346, 112–121, 2007.
Van Meijgaard, E., Van Ulft, L. H., Van De Berg, W. J., Bosveld, F. C., Van Den Hurk, B. J. J. M., Lenderink, G., and Siebesma, A. P.: The KNMI regional atmospheric climate model RACMO, version 2.1 KNMI-publication TR-302 KNMI, de Bilt, The Netherlands, 2008.
Wriedt, G., Van der Velde, M., Aloe, A., and Bouraoui, F.: Estimating irrigation water requirements in Europe, J. Hydrol., 373, 527–544, 2009.
Zhang, Z., Chen, X., Ghadouani, A., and Shi, P.: Modelling hydrological processes influenced by soil, rock and vegetation in a small karst basin of Southwest China, Hydrol. Process., 25, 2456–2470, 2011.

HESSD
9, 1–27, 2012

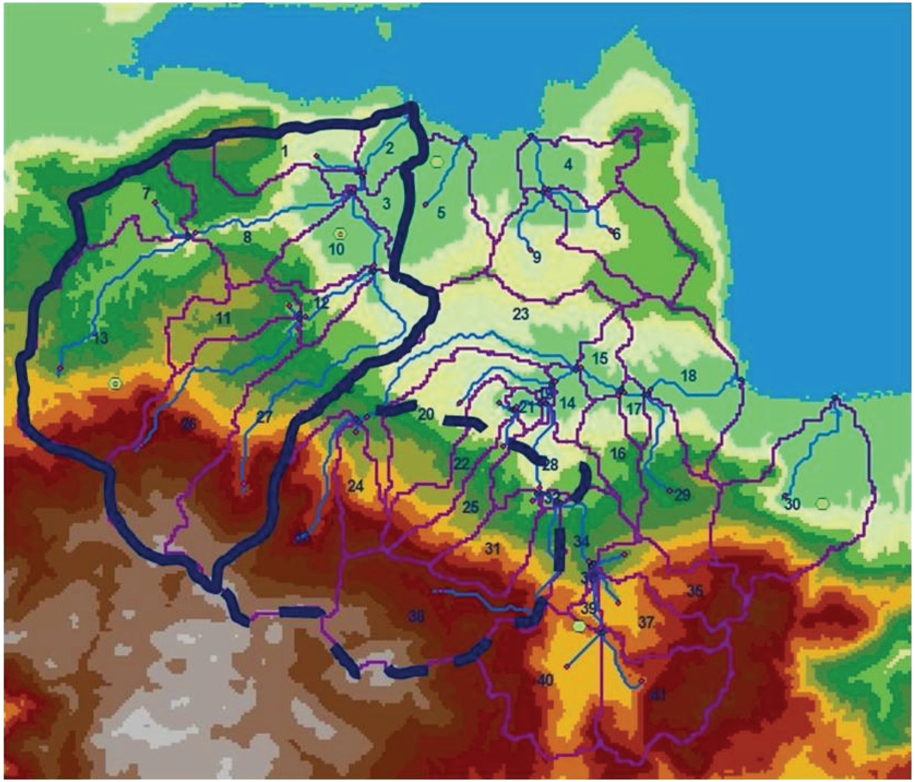

Fig. 1. Digital elevation model delineating the Koiliaris River basin boundary, the model estimated extended karst area and the sub-basins within the watershed.

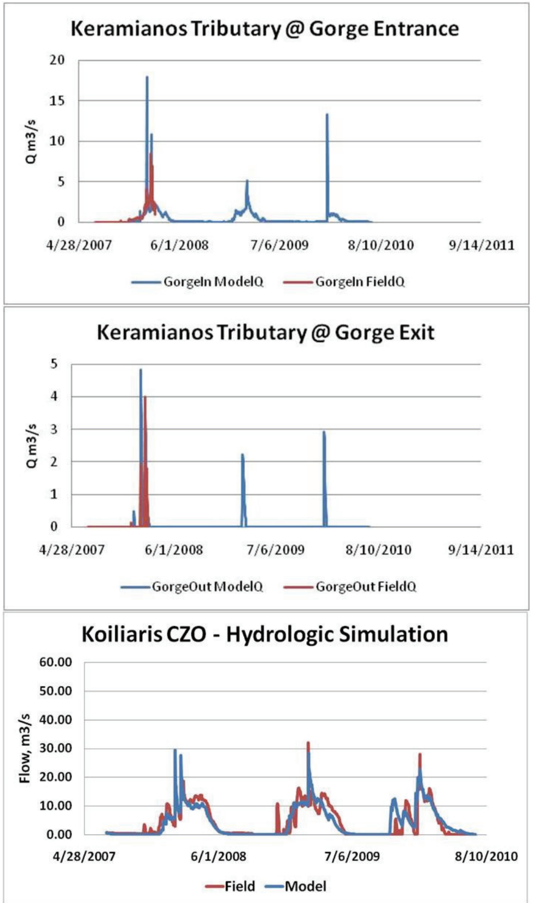

Fig. 2. Comparison of simulated flows with field data **(a)** at the entrance of the gorge, **(b)** the exit of the gorge and **(c)** the basin outlet used for model calibration.

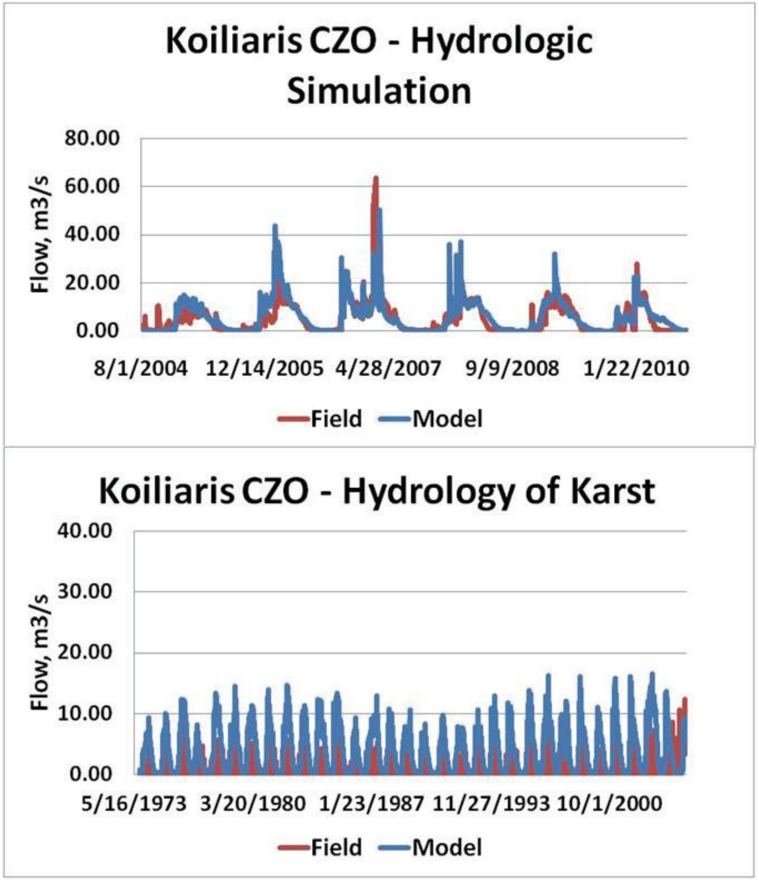

Fig. 3. Comparison of simulated flows with field data **(a)** at the basin outlet used for model verification and **(b)** long term simulation of the hydrology of the karst.

HESSD
9, 1–27, 2012

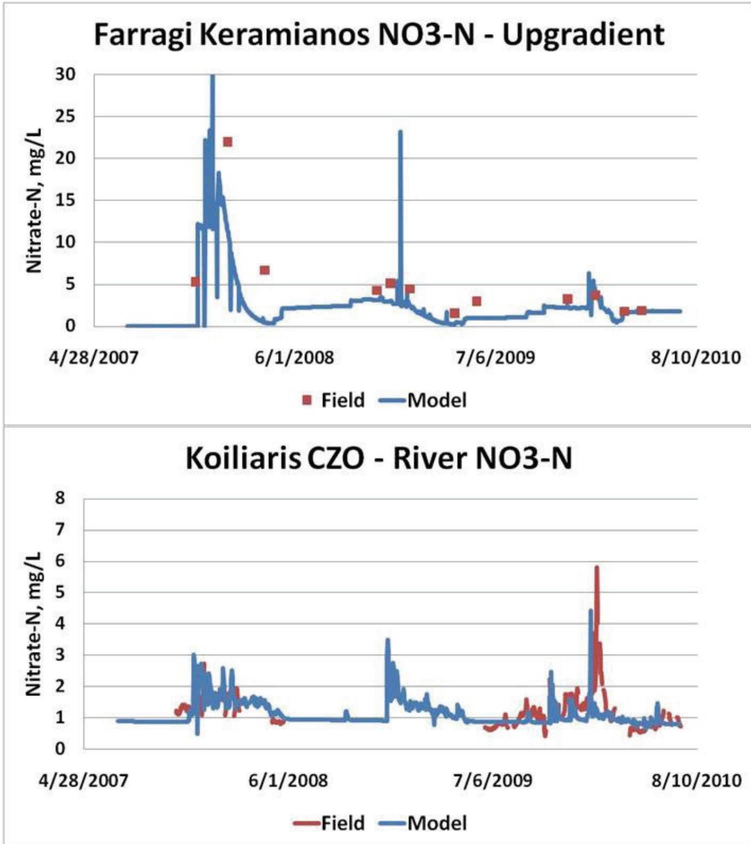

Fig. 4. Comparison of simulated nitrate concentrations with field data **(a)** at the entrance of the gorge and **(b)** the basin outlet used for model calibration.

HESSD
9, 1–27, 2012

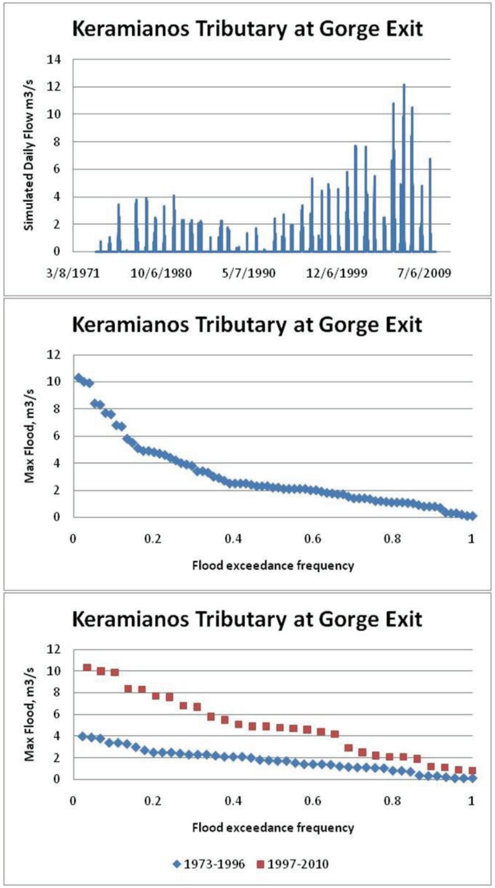

Fig. 5. Flush flood analysis of Keramianos Tributary at the gorge exit. **(a)** Simulated daily flow, **(b)** maximum flow – flood exceedance frequency using all floods (1973–2010), and **(c)** maximum flow – flood exceedance frequencies for 1973–1996 and 1997–2010.

HESSD
9, 1–27, 2012

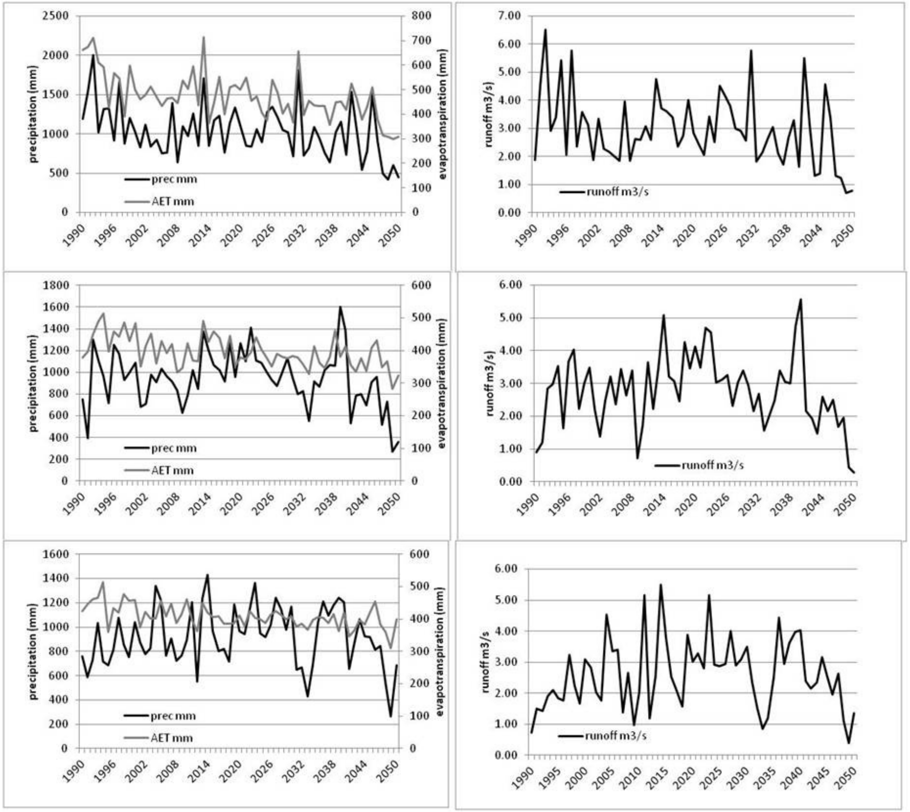

Fig. 6. Predictions of precipitation, ET (left) and flow (right) for Koiliaris River Basin under the **(a)** BCM_RCA, **(b)** ECHAM_RACMO, and **(c)** ECHAM_REMO climate change scenarios for 1990–2050.

HESSD
9, 1–27, 2012

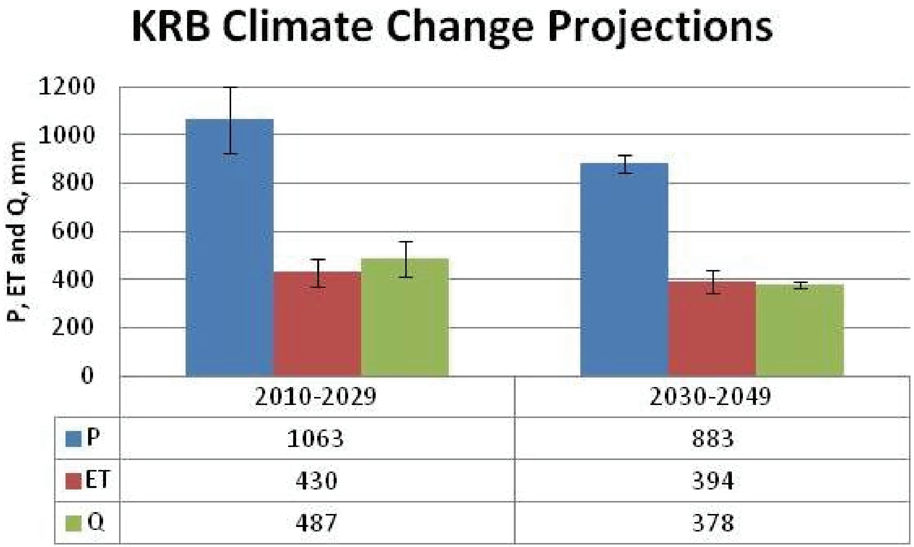

Fig. 7. Predictions of 20-yr average (and standard deviation) precipitation, ET and flow from the three climate change scenarios for Koiliaris River Basin.

HESSD
9, 1–27, 2012